

Metagenomic analysis reveals soil microbiome responses to microplastics and ZnO nanoparticles in an agricultural soil

Jiao Sun ^{a,b}, Weiwei Yang ^a, Mingwei Li ^a, Shuwu Zhang ^a, Yuhuan Sun ^a, Fayuan Wang ^{a,*¹,1}

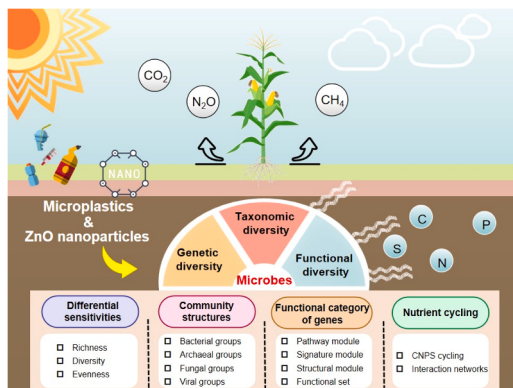
^a College of Environment and Safety Engineering, Qingdao University of Science and Technology, Qingdao, Shandong, 266042, PR China

^b Shandong Vocational College of Science and Technology, Weifang, Shandong 261000, PR China

HIGHLIGHTS

- Metagenomic analysis of soil microbiomes exposed to MPs and nZnO was explored.
- MPs and nZnO synergistically influenced microbial diversity and functions.
- Soil archaea, fungi, and viruses were more sensitive to MPs and nZnO exposure.
- Co-existing MPs mitigated nZnO-induced negative effects on microbial networks.
- High-dose PLA adversely affected fungal communities and microbial interactions.

GRAPHICAL ABSTRACT



ARTICLE INFO

Keywords:
Biodegradable microplastics
Engineered nanoparticles
Nutrient cycling
Soil microbial community
Soil viruses

ABSTRACT

Both microplastics (MPs) and engineered nanoparticles are pervasive emerging contaminants that can produce combined toxicity to terrestrial ecosystems, yet their effects on soil microbiomes remain inadequately understood. Here, metagenomic analysis was employed to investigate the impacts of three common MPs [i.e., polyethylene (PE), polystyrene (PS), and polylactic acid (PLA)] and zinc oxide nanoparticles (nZnO) on soil microbiomes. Both MPs and nZnO significantly altered the taxonomic, genetic, and functional diversity of soil microbes, with distinct effects depending on dosage or type. Archaea, fungi, and viruses exhibited more pronounced responses compared to bacteria. Higher doses of MPs and nZnO reduced gene abundance for nutrient cycles like C degradation and N cycling, but enhanced CO₂ fixation and S metabolism. nZnO consistently decreased the complexity, connectivity, and modularity of microbial networks; however, these negative effects could be mitigated by co-existing MPs, particularly at elevated doses. Notably, PLA (10 %, w/w) exhibited greater harm to fungal communities and increased negative interactions between microbes and nutrient-cycling genes, posing unique risks compared to PE and PS. These findings demonstrate that MPs and nZnO interact

* Corresponding author.

E-mail address: wangfayuan@qust.edu.cn (F. Wang).

¹ ORCID: <http://orcid.org/0000-0003-1345-256X>

synergistically, complicating ecological predictions and emphasizing the need to consider pollutant interactions in ecological risk assessments, particularly for biodegradable MPs.

1. Introduction

The proliferation of plastic waste across various ecosystems has emerged as a critical global concern, drawing the attention of scientists and policymakers alike. Among the diverse forms of plastic pollution, microplastics (MPs) which are defined as plastic particles or fragments with sizes smaller than 5 mm have garnered particular scrutiny due to their widespread presence and potential to cause significant ecological risks globally [1]. Initially identified in marine environments, MPs are now recognized as pervasive pollutants that have infiltrated terrestrial ecosystems, where they adversely affect plants and terrestrial organisms, such as disturbing plant performance [2–4] and disrupting microbial communities and their ecological functions [5–8]. However, the severity and nature of these impacts are highly variable, contingent on the characteristics of MPs and co-existing contaminants [9,10].

Soil ecosystems are among the most biologically diverse environments on earth, hosting a vast variety of microorganisms essential for nutrient cycling, organic matter decomposition, soil structure formation, and plant growth promotion. The diversity, abundance, and activity of these microorganisms are sensitive to environmental changes, including the presence of pollutants like MPs [7,11,12]. In addition, MPs can interact with other co-existing pollutants, posing complex challenges to soil microbial communities [5,13,14]. Previous studies have demonstrated that MPs can alter the composition and diversity of both soil bacteria and fungi [15,16]. However, the extent of these effects is inconsistent, driven by intrinsic differences in microbial composition, functional diversity, and community interactions. Additionally, unique adaptive responses and genetic variability among microbial populations contribute to the distinct reactions observed. The diverse physical and chemical characteristics of MPs, along with their interactions with co-existing contaminants and the leaching of toxic chemicals, further complicate these impacts [5,17]. The co-exposure of MPs and contaminants may produce synergistic, additive, or antagonistic toxicity on soil microorganisms [18,19]. To date, substantial gaps remain in understanding the variable effects of MPs on different soil microbial communities (encompassing bacteria, fungi, archaea, and viruses), necessitating further investigation to validate and deepen our understanding of these interactions.

Nanoparticles, another class of emerging contaminants, pose considerable threats to ecological and biological health due to properties similar to those of MPs [20]. Zinc oxide nanoparticles (nZnO), widely used in sunscreens, cosmetics, paints, and coatings for their unique antimicrobial properties and UV-blocking capabilities [21], are increasingly present in terrestrial environments due to wastewater irrigation, atmospheric deposition, and the disposal of ZnO-containing products. In soil, nZnO exert antimicrobial effects by generating reactive oxygen species (ROS), which can disrupt cell membranes, damage cellular components, and interfere with critical biochemical processes [22,23]. The co-occurrence of nZnO and MPs in agroecosystems may lead to different bioavailability and toxicity profiles, potentially resulting in synergistic or antagonistic effects on microbial communities. However, the specific interactions between MPs and nZnO, and their consequences remain uncertain and are yet to be verified through in-depth study.

Previous research has demonstrated that MPs and nZnO can induce substantial alterations in soil properties and the performance of plants and soil fauna [24–27], particularly the structure and diversity of symbiotic arbuscular mycorrhizal fungi [24] and rhizosphere bacteria [25]. However, these studies did not involve other microbial members with important ecological functions, such as soil fungi, archaea, and viruses. Furthermore, most studies focused only on the type of MPs. We

hypothesize that exposure to MPs and nZnO, both individually and jointly, induces changes in taxonomic composition, functional diversity, and ecological interactions within the soil microbiomes. To test this hypothesis, the objectives of this study were to: (i) investigate the individual and combined effects of MPs and nZnO on microbial taxonomic diversity and community structure, (ii) assess the functional shifts in microbial communities and (iii) examine the complexity and stability of microbial interaction networks under these treatments. Specifically, two conventional non-degradable plastics—polyethylene (PE) and polystyrene (PS)—along with biodegradable polylactic acid (PLA), were selected to represent the most prevalent environmental plastics. The results can help to recognize their integrated risks from the perspective of soil microbiomes, which are essential for maintaining soil health and biodiversity and ensure sustainable agricultural productivity.

2. Material and methods

2.1. MPs and nZnO

Three types of MPs commonly used in agricultural production were selected for this study, i.e., high-density PE, PS, and PLA. PE and PS were chosen due to their widespread presence in agricultural settings, while PLA, known for its environmentally friendly and biodegradable properties, is frequently used as an alternative in agricultural films. MPs used in the experiments were manually sieved to ensure that particle sizes ranged between 100 and 154 µm, a range considered environmentally realistic based on observations in various farmlands across China [28]. The characteristics of the three types of MPs were detailed in Table S1 and verified using Fourier transform infrared spectroscopy (FTIR) (Fig. S1), which were described in our previous studies [24]. nZnO were purchased from Shanghai Macklin Biochemical Co., Ltd, and were characterized as spherical or irregular nanoparticles with the following properties: purity of 99.9 %, average particle size of 30 ± 10 nm, zeta potential of +1.13 mV, and average surface area of $39.25 \text{ m}^2/\text{g}$, as depicted in Fig. S2.

2.2. Soil

The test soil was collected from a local agricultural field. The fundamental physicochemical properties were summarized in Table S2. The detailed information was described in our previous research [24].

2.3. Experimental design and procedure

A trifactorial experiment was designed, incorporating three types of MPs (PE, PS, and PLA), four different addition doses (0, 0.1 %, 1 %, and 10 %, w/w), and three nZnO doses (0, 50, and 500 mg ZnO/kg soil). As outlined in Table S3, a total of 30 unique sample groups (29 treatments and one control) were prepared, with each group replicated three times, resulting in 90 soil samples for subsequent analysis. Considering that mulching films particularly biodegradable ones are not completely recovered, the plastic residues are likely to accumulate unevenly in the field and plasisphere may become hotspots of MPs. Based on the environmental concentrations of MPs in soils [29] and previous studies [30–33], the doses of MPs were set at 0.1 % and 1 % (w/w) representing environmentally relevant concentrations and 10 % (w/w) representing soil plastic hotspots with high MPs levels. The nZnO levels were designed based on prior research [24,34].

To minimize aggregation and enhance homogeneity, the accurately weighed air-dried soil (< 2 mm), MPs, and nZnO for each treatment were placed into a clean enamel tray, and then thoroughly mixed by

manual stirring for about 20 minutes. The treated soil was then transferred into polyethylene pots, each containing 950 g of the soil mixture. To simulate crop cultivation, maize (*Zea mays* L.) was selected as the test plant because of its world-wide cultivation. Surface sterilized maize seeds (variety Wannuoysiiao) were sown and ten seedlings were retained in each pot [24]. The pots were then randomly arranged in a controlled plant growth chamber set to a 12-hour light/12-hour dark cycle, with light intensity of 10,000 lux, temperature 25–28 °C during the day and 20–23 °C at night, and the relative humidity of 50 %–55 %. To ensure optimal growth conditions, deionized water was added daily to maintain soil moisture at approximately 70 % of water-holding capacity. One month post-sowing, the aerial parts of the plants were cut off for further analysis. The entire pot of soil was transferred into an enamel tray for root collection and soil sampling. Large roots were manually taken with tweezers and the remaining capillary roots were collected by sieving. To minimize spatial variability and potential biases in microbial community analysis, the soil was thoroughly mixed again to ensure homogeneity. Approximately 10 g of fresh soil was taken and stored at –80°C for subsequent DNA extraction and metagenomic analysis. Because the results on plant biomass and Zn concentrations have been partly reported in our previous paper [24], here we mainly address the response of soil bacteria, fungi, archaea, and viruses by employing metagenomic analysis.

2.4. DNA extraction and sequencing

A total of 90 samples, comprising 29 treatments and one control, with each treatment replicated three times, were prepared. Genomic DNA was extracted from each sample using the TIANamp Soil DNA Kits (Tiangen Biotech, Beijing, China), adhering to the manufacturer's protocol. Importantly, MPs were retained in the soil and not removed prior to DNA extraction. The quality and quantity of the extracted DNA were assessed using a NanoDrop-2000 spectrophotometer (Thermo Fisher Scientific, MA, USA) and 2 % agarose gel electrophoresis, respectively, as detailed in our previous study.

Metagenomics DNA libraries were prepared using the Illumina DNA Prep Kit (Illumina, San Diego, CA, USA) to generate 300-bp paired-end reads. Fragmented DNA was end-repaired and ligated to sequencing adapters, and paired-end sequencing was performed on the Illumina HiSeq 2500 platform by Sangon Biotech (Shanghai) Co. Ltd, China. Raw sequencing reads were processed to remove low-quality sequences and adapters using Sickle. Clean reads were then assembled using de Bruijn graph-based assembler SOAPdenovo v1.06 to generate contigs. The assembled contigs were further analyzed to identify microbial species and functional genes. Raw sequencing data have been deposited in the NCBI Sequence Read Archive (SRA) under Bioproject ID PRJNA1223538.

2.5. Gene taxonomic classification and functional annotation

Open reading frames (ORFs) from each assembled contig were predicted using Prodigal, generating the corresponding protein sequences. Genes with 95 % sequence identity were clustered and mapped to the representative sequences using CD-HIT. Gene abundance in individual samples was calculated by normalizing the read count per gene to the total number of reads in each sample. The protein sequences derived from the assembled ORFs were annotated by searching against the KEGG database using an e-value cutoff of 1e-5 to ensure significant matches. KEGG pathway mapping was performed by aligning sample sequences to KEGG pathways, and pathway module analysis was conducted using MEGAN v6, which facilitated the visualization and interpretation of functional data within the context of KEGG pathways.

2.6. Statistical analysis

Data are presented as the mean ± standard deviation. Main effects

and interaction effects across the three independent variables (MPs type, MPs dose, and nZnO) were compared using analysis of variance (ANOVA), followed by Duncan's multiple range test to identify statistically significant differences between sample groups. Normality and homogeneity of variances were assessed, and Kruskal–Wallis tests were employed when these assumptions were not met. Correlation analysis was conducted using Pearson or Spearman correlation coefficients, depending on the data distribution. All statistical analyses were performed using IBM SPSS Statistics v26 (SPSS Inc, Chicago, USA) and RStudio v4.3.0 (RStudio Inc., USA), with a p-value of < 0.05 considered statistically significant. Additional analyses, including the Mantel test, variance partitioning analysis (VPA), and co-network modeling, were conducted using RStudio software with the linkET, tidyverse, vegan, and Hmisc packages. Data visualization and interpretation were facilitated using Origin v2019 (OriginLab Corporation, Northampton, USA), Gephi v0.10, and various RStudio packages (ggridges, ggplot2, RColorBrewer, and igraph).

3. Results

3.1. Characteristics of soil microbial communities

The investigation into the soil microbial characteristics revealed distinct variations in alpha diversity indices across different microbial groups, including bacteria, archaea, fungi, and viruses. Key metrics, richness (observed species), diversity (Shannon's H), and evenness (Simpson 1-D) were significantly influenced by the presence of MPs, nZnO, and their interactions, as detailed in Tables S3–S7. Fig. 1 illustrates how these indices varied.

3.1.1. Microbial community richness (observed species)

Bacterial richness remained relatively high across all treatments, with only slight variations observed. However, elevated doses of MPs (10 %, w/w) and nZnO (500 mg/kg) led to a slight decline in richness, particularly in the PLA treatment. Trends in archaeal richness showed a more pronounced decrease under high doses of MPs and nZnO, especially with PLA. Interestingly, archaeal richness exhibited a positive correlation with MPs accumulation at lower nZnO levels (0 or 50 mg/kg), which reversed at higher nZnO levels (500 mg/kg), indicating a complex interaction where the benefits of MPs are negated by higher nZnO levels. Fungal richness was also negatively impacted by higher doses of MPs and nZnO, with significant reductions observed under certain treatments. Although all microbial groups were affected by MPs and nZnO, viral communities appeared particularly sensitive to these pollutants at elevated doses. Notably, the presence of nZnO seemed to mitigate the adverse effects of MPs on viral richness.

3.1.2. Microbial community diversity (Shannon's H)

Shannon's diversity index for bacteria showed a slight decrease under high doses of MPs and nZnO. Remarkably, bacterial diversity was notably elevated in PLA treatments compared to PE and PS treatments, suggesting that biodegradable MPs might have a less detrimental effect on bacterial diversity compared to conventional MPs, especially at elevated doses. In contrast, archaeal diversity indices increased with higher doses of MPs or nZnO, with the highest diversity values consistently observed in 10 % PLA treatments, regardless of nZnO addition. Fungal communities exhibited the most significant decline in diversity with increasing doses of MPs and nZnO, particularly under 10 % PLA exposure, indicating that high doses of biodegradable MPs could severely impact fungal diversity. Viral diversity also decreases under high pollutant conditions, similar to richness.

3.1.3. Microbial community evenness (Simpson 1-D)

Bacterial evenness remained relatively stable but increased slightly in the presence of MPs and nZnO. Co-exposure to MPs mitigated the negative effects of nZnO on bacterial evenness, with the highest

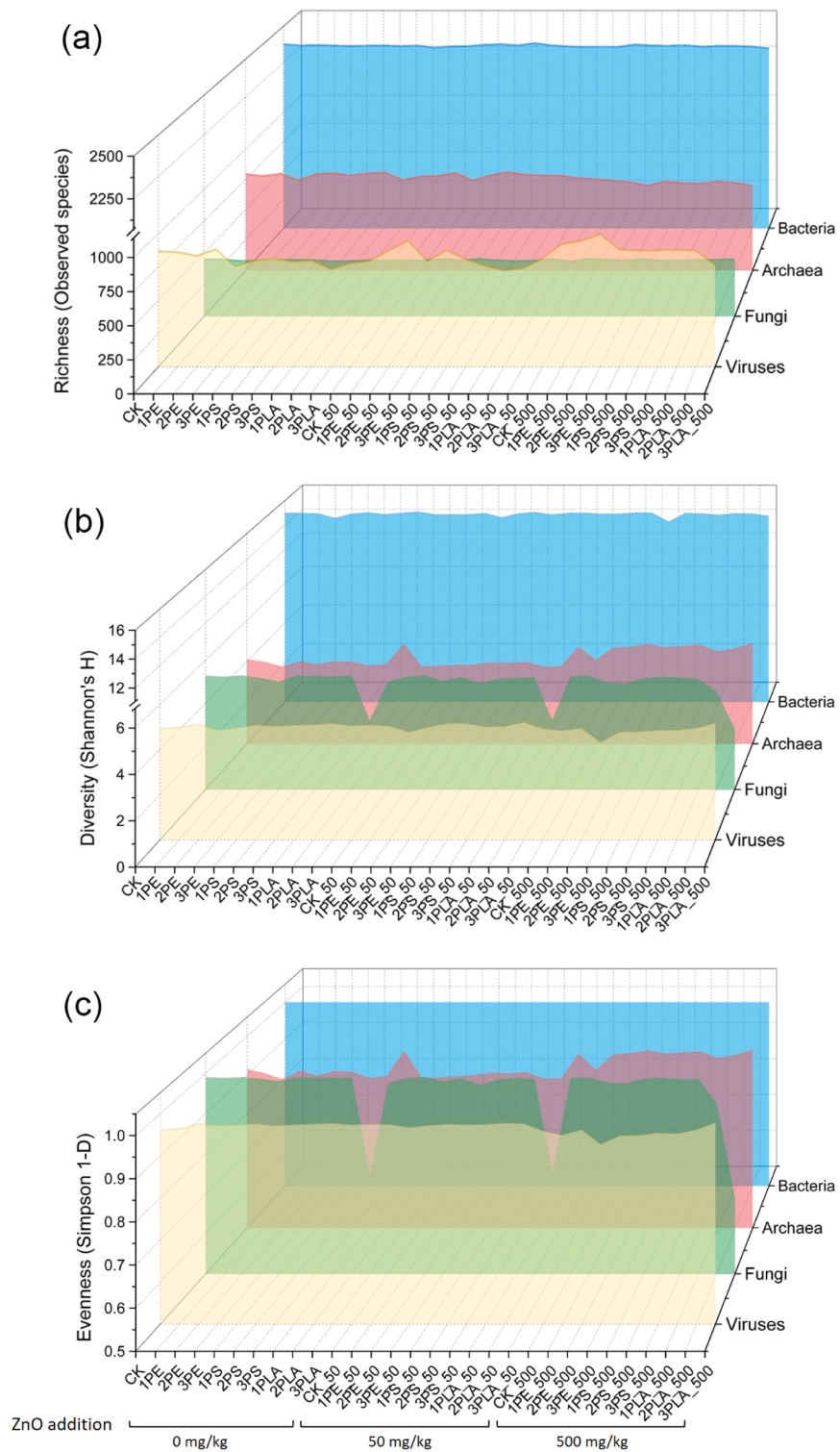


Fig. 1. Richness (a), Diversity (b), and Evenness (c) index of different microbial communities exposed to MPs and nZnO, either individually or in combination. CK represents the control treatment without MPs or nZnO. The numbers 1, 2, and 3 in front of PE, PS, and PLA represent the dose of 0.1 %, 1 %, and 10 % (w/w), respectively, while 50 and 500 represent to treatment with 50 and 500 mg/kg nZnO, respectively.

evenness observed in the 10 % (w/w) MPs and 500 mg/kg nZnO treatments, particularly with PLA. Archaeal evenness followed a similar pattern to diversity, increasing under high doses of nZnO and MPs, especially with PLA. Fungal evenness remained stable across most treatments, with minor reductions under high-stress conditions, but significant reductions were observed with high-dose PLA and nZnO combinations. Viral evenness exhibited the greatest variability, with

significant reductions at the highest nZnO level (500 mg/kg), particularly in combination with MPs, indicating that pollutant stress disproportionately affects certain viral taxa.

3.2. Composition of soil microbial communities

3.2.1. Composition of bacterial communities

Microbial communities were classified into distinct taxonomic levels, encompassing 107 phyla, 378 orders, 730 families, 2466 genera, and 15,985 species. Bacteria dominated in terms of relative abundance, comprising 84.5 % of the total microbial communities, followed by archaea (0.9 %), fungi (0.2 %), and viruses (0.1 %). Fig. 2a and 2b depict the bacterial community structure at the phylum and genus level, respectively. Across all treatments, the most abundant phyla were Proteobacteria, Actinobacteria, and Acidobacteria, collectively contributing between 70.1 % and 79.5 % of the total bacterial communities. Proteobacteria emerged as the most prevalent phylum, with a relative abundance ranging from 23.3 % to 46.5 %. This phylum exhibited increased sensitivity to variations in MPs types, with decreases under high-dose PE and PS exposure, but an increase with PLA exposure, peaking at 10 % addition. Conversely, Actinobacteria demonstrated an opposite trend, responding positively to higher levels of conventional MPs (PE and PS), as well as to nZnO and their combined treatments. When treated with nZnO alone, the relative abundances of dominant phyla remained largely unchanged, indicating minimal impact on bacterial community richness and structure in the absence of MPs.

At the genus level, the impacts of MPs and nZnO on soil bacterial communities varied based on the type and dose of MPs and the presence of nZnO. Key genera affected included *Sphingomonas*, *Streptomyces*, *Gemmattirosa*, *Nocardioides*, and *Bradyrhizobium*. *Sphingomonas* and *Gemmattirosa* demonstrated general resilience to MPs and nZnO, with *Sphingomonas* exhibiting a notably higher relative abundance under PS exposure, especially at 0.1 % addition. *Streptomyces* tended to increase with higher MPs doses, particularly PLA, but decreased with elevated nZnO levels when co-occurring with PS and PE. For the genera *Nocardioides* and *Bradyrhizobium*, the adverse effects of high-dose nZnO on their abundances were contingent upon the type of MPs.

3.2.2. Composition of archaeal, fungal, and viral communities

Fig. 2c and d present the relative abundance of archaea, fungi, and viruses under different treatments. Among archaea, Thaumarchaeota and Euryarchaeota were the dominant phyla. The abundance of Thaumarchaeota was highly dependent on high-dose nZnO addition, especially in the presence of PE and PS. Euryarchaeota displayed a similar trend, consistently decreasing as nZnO doses increased, but peaking at 0.1 % and 1 % MPs exposure in most treatments. In fungal communities, Ascomycota and Basidiomycota emerged as the dominant phyla, with their abundances varying significantly with MPs type. Ascomycota showed an observable increase with PLA addition, while remaining relatively stable across other treatments, even under 500 mg/kg nZnO exposure. Meanwhile, Viruses noname experienced a significant increase in abundance when exposed to elevated doses of nZnO, particularly in combination with PE and PS.

For the dominant archaeal genus, *Nitrososphaera* responded negatively to increasing doses of nZnO, with a decline in abundance upon PE and PS addition. The methanogenic archaeal genus *Methanosaerina* maintained consistent levels with minor fluctuations. Within fungal communities, significant increases in the genera *Talaromyces* and *Exophiala* were observed only with 10 % PLA exposure, while *Trichoderma* and *Rhizopus* remained relatively stable across treatments, consistently ranking as dominant fungal genera. It is noteworthy that higher nZnO addition positively impacted the abundances of the dominant viral genera *Siphoviridae noname* and *Viruses noname*, with further improvements observed when combined with traditional MPs (PE and PS).

3.2.3. Impact of MPs and nZnO on overall soil microbial community composition

VPA analysis, depicted in Fig. 2e, highlights that MPs, nZnO, and their interactions contribute significantly to changes in the community structures of soil microbes. Among these factors, nZnO dose (16.8 %)

accounted for the greatest proportion of variation, followed by MPs dose (11.1 %) and MPs type (6.1 %). Interactions between these factors were also contributed, with the two-way interaction between MPs type and dose explaining 0.4 % of the variation, and the three-way interaction involving MPs type, MPs dose, and nZnO accounting for 0.02 % of the total variation in microbial community structure. Furthermore, as illustrated in Fig. S3, both hierarchical clustering dendrogram and principal coordinates analysis (PCoA) confirmed the pronounced effects of MPs type, MPs dose, and nZnO on the composition and structure of soil microbial community clusters. Notably, groups subjected to higher doses of nZnO (500 mg/kg) exhibited distinct separations from those exposed to lower doses (0 and 50 mg/kg), indicating a substantial impact of high-dose nZnO on the microbial community clustering, consistent with the VPA analysis. Moreover, each type of MPs (PE, PS, and PLA) exposure showed unique clustering patterns, highlighting the pivotal role of MPs type in shaping the structural outcomes of soil microbial communities.

3.3. Responses of functional categories of genes within soil microbial communities

Metagenomic sequencing and subsequent annotation provided comprehensive insights into the functional categories of genes within soil microbial community. Pearson correlation analyses (Fig. 3a), Mantel test (Fig. 3b), and ANOVA analyses (Table S8) were conducted to assess the impact of MPs type, MPs dose, nZnO, and their interactions on the relative abundance of potential functional categories as shown in Fig. 3 and Table S8. Specifically, MPs dose showed strong positive correlations with pathway modules related to carbohydrate and lipid metabolism, nucleotide and amino acid metabolism, and secondary metabolism, while negatively affecting other modules. MPs type also influenced various functional modules—particularly the pathway module, structural module, and functional sets—mostly exerting positive effects. In contrast, nZnO exhibited significant negative effects on both the structural and functional modules, which implies a suppressive effect on microbial activities related to energy metabolism and genetic processing.

In the pathway module, carbohydrate and lipid metabolism pathways were particularly sensitive to both MPs and nZnO, as well as their interactions, with pronounced effects observed across several sub-categories. For central carbohydrate metabolism, both MPs dose ($F=29.79^{***}$) and nZnO ($F=11.83^{***}$) exhibited significant impacts, indicating that the dose of these pollutants plays a critical role in altering carbohydrate processing within microbial communities. The interaction between MPs type and nZnO was also significant ($F=5.68^{**}$). In the fatty acid metabolism pathway, MPs dose emerged as the most influential factor ($F=314.16^{***}$), highlighting a strong dose-dependent response. Significant effects were also observed for MPs type ($F=52.71^{***}$) and its interactions with other factors, particularly nZnO ($F=34.07^{***}$). Energy metabolism pathways, such as carbon fixation and sulfur metabolism, were also significantly affected. Both MPs dose and nZnO negatively influenced carbon fixation ($F=19.79^{***}$ and $F=22.16^{***}$, respectively), while sulfur metabolism showed extremely high significance levels across all factors, with MPs type having the highest impact ($F=191.50^{***}$). The interaction between MPs type and dose ($F=104.05^{***}$) further emphasizes the compounded effects these pollutants exert on critical energy-producing processes. In contrast, nucleotide and amino acid metabolism pathways, particularly branched-chain amino acid metabolism and cysteine and methionine metabolism, demonstrated positive correlations with MPs type and dose. MPs type had a profound effect on branched-chain amino acid metabolism ($F=187.11^{***}$), while interactions with MPs dose and nZnO were also significant. Secondary metabolism also showed significant positive correlations with MPs type and dose, as well as nZnO. Pathways related to aromatics degradation were particularly sensitive to MPs, with MPs dose showing an exceptionally high F value ($F=283.33^{***}$), suggesting

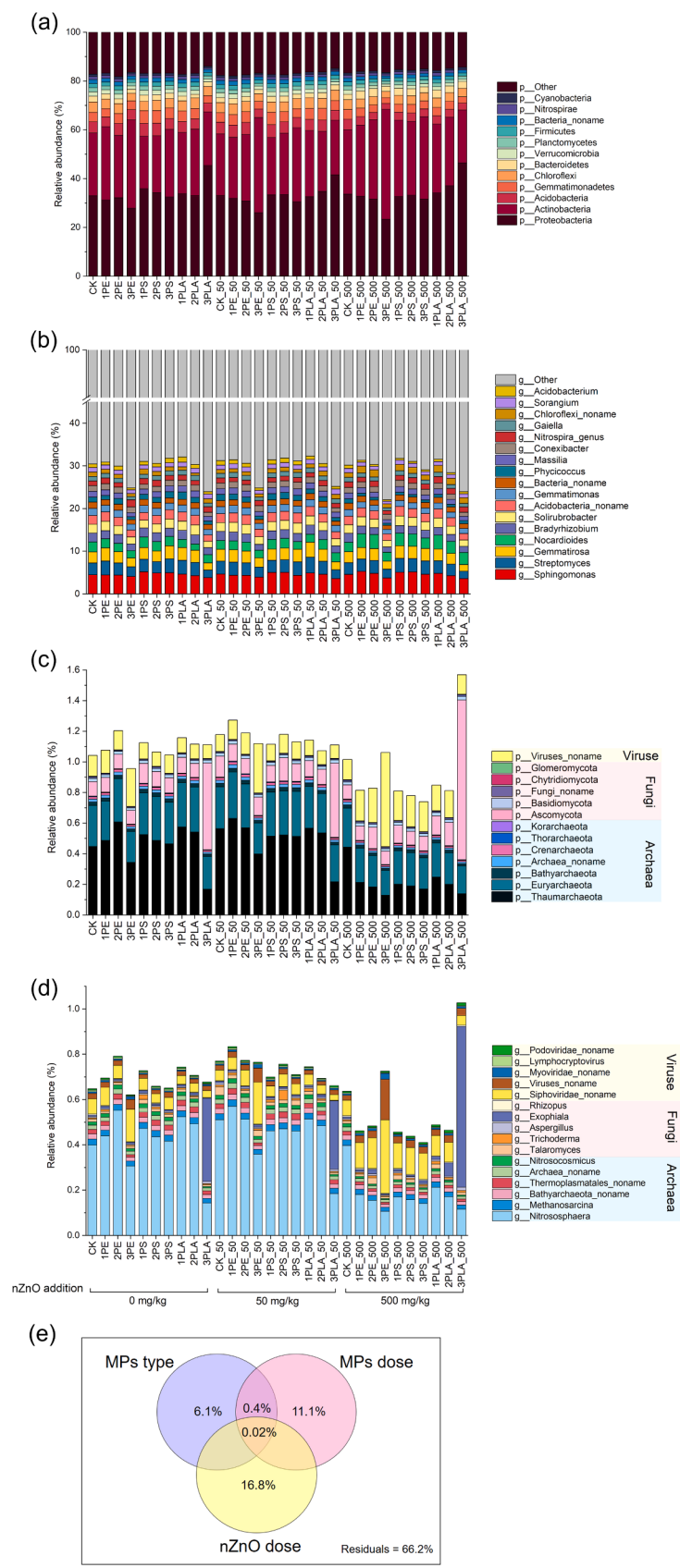


Fig. 2. The terrestrial microbial communities exposed to MPs, nZnO, and their combination, shown by (a) bacterial phyla, (b) bacterial genera, (c) archaeal, fungal, and viral phyla, (d) archaeal, fungal, and viral genera, and (e) variance partitioning analysis (VPA) of microbial community structures influenced by MP type, MP dose, and nZnO dose. Explanatory values below zero are not displayed. CK represents the control treatment without MPs or nZnO. The numbers 1, 2, and 3 in front of PE, PS, and PLA represent the dose of 0.1 %, 1 %, and 10 % (w/w), respectively, while 50 and 500 represent treatment with 50 and 500 mg/kg nZnO, respectively.

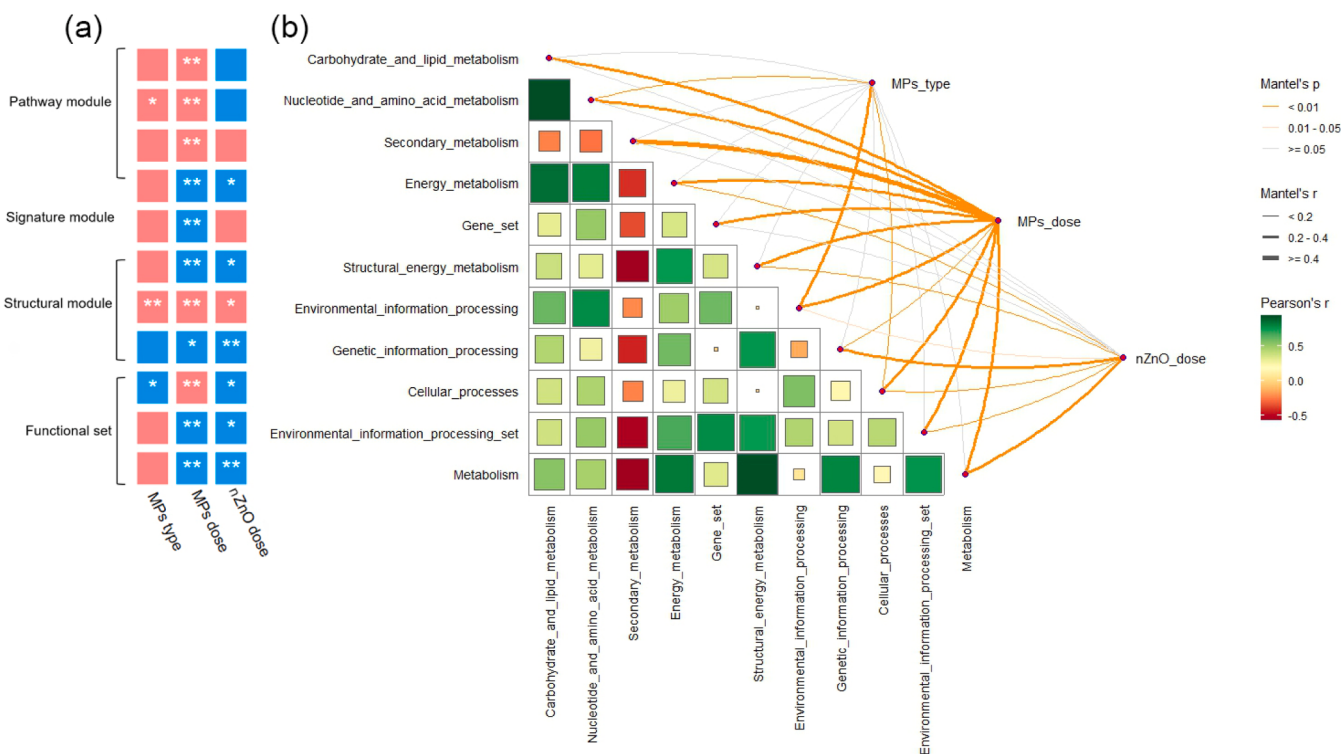


Fig. 3. Pearson correlation analyses (a) and Mantel test (b) for the relative abundance of functional genes influenced by MPs type, MPs dose, nZnO, and their interactions. In Fig. 3a, blue and red colors represent positive and negative correlations, respectively. Significance levels are denoted as follows: $P < 0.05$ (*), $P < 0.01$ (**), $P < 0.001$ (***)]. In Fig. 3b, the grey lines indicates no significance ($P \geq 0.05$), the lemon yellow line denotes significance ($0.01 \leq P < 0.05$), and the orange yellow line indicates significance ($P < 0.01$). The width of the line reflects the strength of the different correlations, while red and green squares represent the correlation strength between two indicators.

that the degradation of aromatic compounds, often linked to the breakdown of complex organic pollutants, was strongly impacted by the presence and dose of MPs. Similarly, the biosynthesis of secondary metabolites pathway was significantly affected by nZnO ($F=36.43^{***}$), and the interaction between MPs type and dose ($F=44.81^{***}$).

In the signature module, gene sets related to drug resistance, metabolic capacity, and pathogenicity also demonstrated significant responses to MPs and nZnO treatments. MPs dose and its interaction with other factors significantly influenced drug resistance ($F=26.83^{**}$ and $F=28.14^{**}$, respectively), suggesting that environmental pollutants may enhance the spread of antibiotic resistance within microbial communities.

Finally, structural complex transportation pathways, including structural energy metabolism, environmental information processing systems, and genetic information processing, demonstrated significant correlations with all three factors (MPs type, dose, and nZnO). However, the latter two showed completely opposite correlations with these stressors. Notably, MPs dose had a pronounced impact on ATP synthesis ($F=69.42^{***}$), a critical pathway for cellular energy production, while environmental information processing pathways, such as drug efflux transporter/pump, also showed significant responses, particularly in relation to MPs type ($F=72.32^{***}$) and its interactions with nZnO ($F=35.84^{***}$).

3.4. Responses of nutrient cycling genes within soil microbial communities

3.4.1. Relative abundances

A total of 81 genes were identified through metagenomic sequencing and annotation, playing key roles in C degradation, C fixation, N cycling, P cycling, S cycling, and pathogenicity. The heatmap analysis presented in Fig. 4 visualizes the relative abundance and activity of these genes across different treatments.

These functional genes exhibited varying levels of abundance across treatments. Genes involved in C degradation exhibited varying levels of relative abundance, with those associated with starch and cellulose breakdown (*AMY/amyA/malS, bglB, bulX*), hemicellulose degradation (*abfA, xynA*), and lignin decomposition (*ligK/galC*), showing diminished abundance under the combined effects of MPs and high-nZnO levels, especially in the presence of PLA. Similarly, genes associated with C fixation, such as *acsA, assA*, and *rbcL* (both involved in the Calvin cycle for CO₂ conversion), exhibited a marked reduction under MPs exposure, particularly at higher nZnO doses. Interestingly, *korA/corA/oforA* genes, encoding key enzymes in CO₂ fixation, demonstrated an opposite trend.

Associated with N cycling, N₂ fixation genes (*nifD, nifK*, and *nifH*), which encode nitrogenase, were less abundant under elevated nZnO and PLA levels, indicating a stimulatory response. Furthermore, genes encoding enzymes involved in ammonia oxidation (*pmoA*), nitrate reduction (*narH/narZ/nrxA*), nitrite reduction (*nirS*), and nitrous oxide reduction (*nosZ*) showed increased abundance in response to higher nZnO doses, indicating a particular sensitivity of N₂ fixation, nitrification, and denitrification processes to these conditions. For P cycling genes, genes such as *phoD, ppK*, and *phnK*, displayed higher abundance under lower nZnO addition, implying that high-dose nZnO might inhibit phosphorous solubilization and mobilization processes. Conversely, S cycling genes demonstrated a distinct response, with increased relative abundance observed under high-level nZnO and MPs exposure, suggesting that sulfur metabolism may be activated as a microbial response to detoxify excess sulfur compounds or maintain sulfur homeostasis under stress conditions. Lastly, regarding pathogenicity-related genes, genes involved in bacterial virulence factors, such as *hlyB, cyaC, cyaA, virB11, cagA*, and *yscC/sctC/ssaC*, showed higher abundance under higher nZnO addition (500 mg/kg) and co-existing to specific MPs types, particularly PLA.

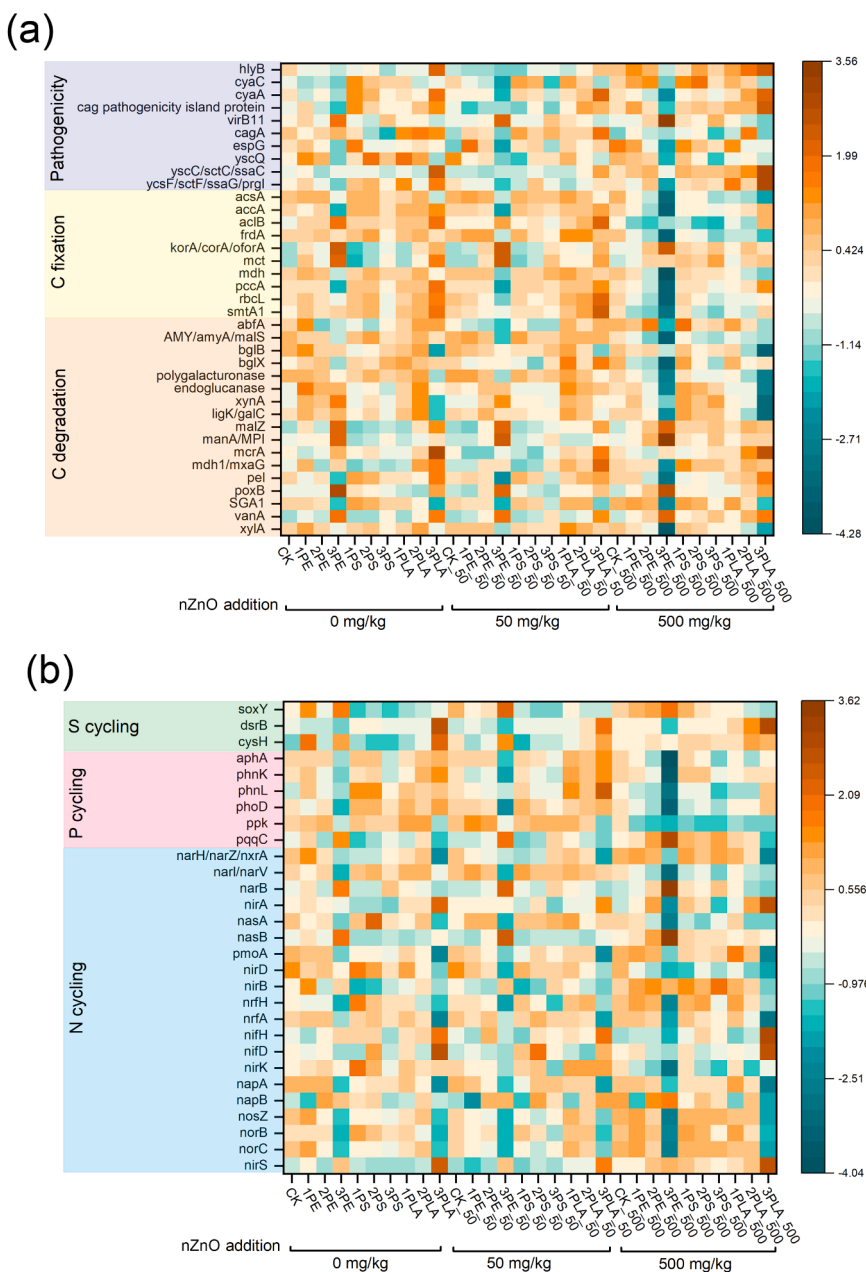


Fig. 4. Heatmaps depicting the relative abundance of functional genes involved in (a) C degradation, C fixation, pathogenicity, and (b) N cycling, P cycling, and S cycling. CK represents the control treatment without MPs or nZnO. The numbers 1, 2, and 3 in front of PE, PS, and PLA represent the dose of 0.1 %, 1 %, and 10 % (w/w), respectively, while 50 and 500 represent to treatment with 50 and 500 mg/kg nZnO, respectively.

3.4.2. Key drivers of variance

As shown by the VPA analysis in Fig. S4, the contributions of MPs type, MPs dose, nZnO, and their interactions with the observed changes in the 81 functional gene profiles were assessed. The nZnO dose was the most significant contributor, accounting for 14.3 % of the variance in these functional gene profiles. MPs dose also had a substantial impact, contributing 9.7 % to the total variance, while MPs type contributed 9.3 %. The interaction between MPs type and dose accounted for 0.02 % of the variance, and the interaction between MPs type and nZnO dose contributed 0.01 %. Furthermore, the three-way interaction among MPs type, MPs dose, and nZnO dose contributes minimally (0.01 %) to the variance. These interactions align with the heatmap analysis results, indicating that the combined effects of MPs and nZnO on microbial genes associated with C, N, P, and S cycling, as well as pathogenicity, involve more complex dynamics that extend beyond mere additive

effects.

3.4.3. Microbial interaction networks under various treatments

Fig. 5a showcases interaction networks derived from metagenomic sequencing data, illustrating the relationships between microbes and the 81 functional genes involved in C, N, P, and S cycling, as well as pathogenicity (human disease) within soil microbial communities. These ecological networks were constructed under varying dosages of MPs and nZnO exposure. Fig. 5b quantifies network characteristics through metrics such as total nodes, links, modularity, path lengths, and weighted degrees.

The control network, without MPs or nZnO addition, exhibited a highly interconnected structure, characterized by a dense web of interactions between microbial communities and functional genes. Central nodes in the CK network represented key genes involved in C fixation, N

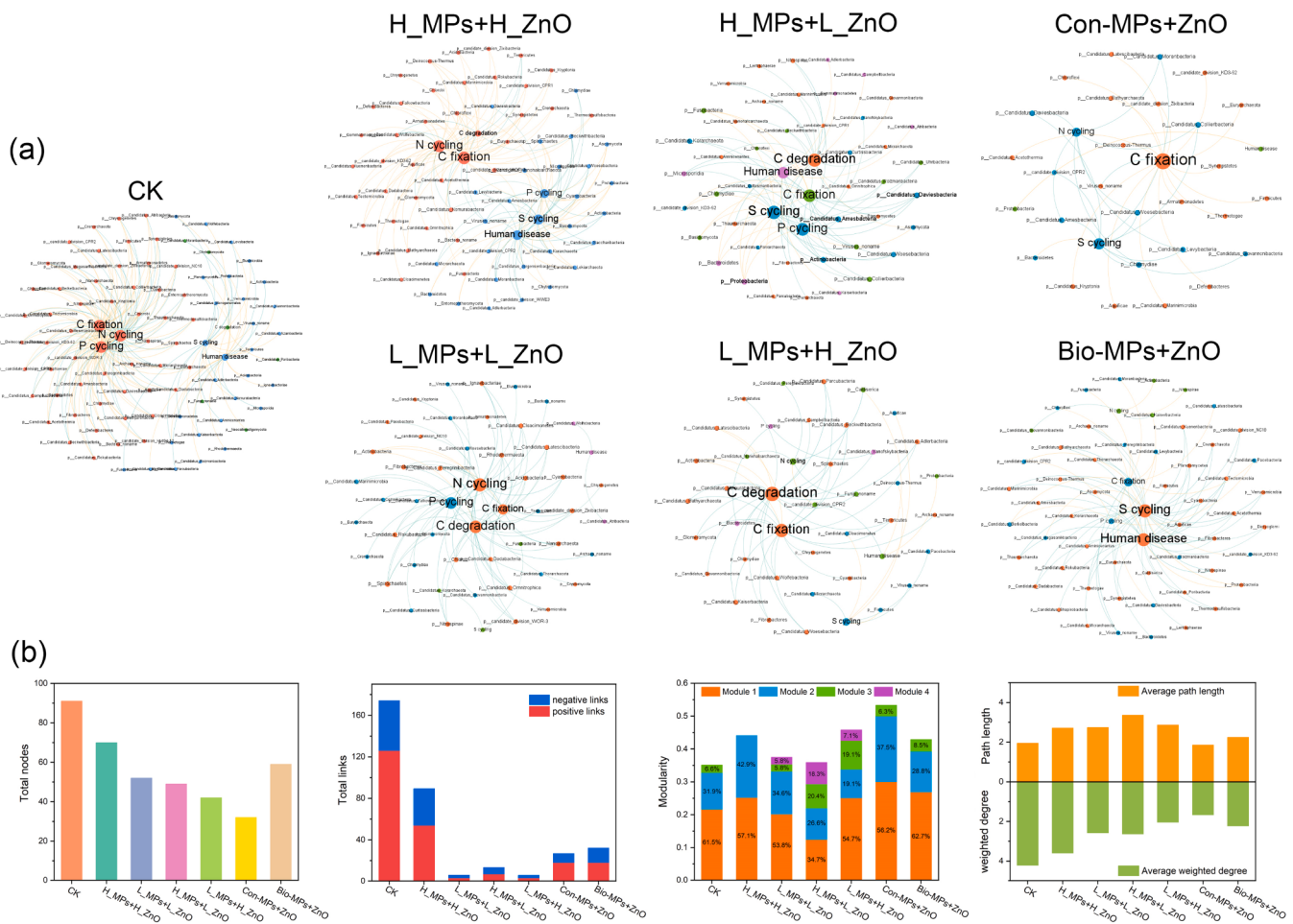


Fig. 5. Microbial interaction networks of microbes and functional genes involved in C, N, P, and S cycling, as well as pathogenicity (human disease). (a) Microbial interaction networks; (b) Topological parameters of microbial interaction networks. CK represents the control treatment without MPs or nZnO. The uppercase letter L and H in front of MPs indicate the dose of 0.1 % and 10 % (w/w), respectively, while L and H preceding nZnO represent treatments with 50 and 500 mg/kg nZnO, respectively. Con-MPs and Bio-MPs refer to conventional MPs (PE and PS) and biodegradable MPs (PLA), respectively.

cycling, and P cycling, which are critical for maintaining soil health and nutrient balance. However, under high-dose of MPs and nZnO co-exposure (H_MPs + H_nZnO), the network became more fragmented, with fewer interactions and an increase in negative links. Central functions, such as C degradation and N cycling, appeared particularly affected, with more interactions confined within the microbial communities. Additionally, human disease-related genes showed greater abundance and more connections with soil microbes compared to the CK network. Conversely, the low-dose MPs and nZnO network (L_MPs + L_nZnO) displayed a simpler and less connected structure, with fewer nodes and links compared to the high-dose treatment, though it exhibited higher modularity. Interactions among key functions, like C degradation, C fixation, as well as P and N cycling, were preserved but demonstrated increased antagonistic connections with soil microbes, indicating a less complex and potentially more unstable microbial community under low-stress conditions.

Under high-dose MPs were combined with low-dose nZnO (H_MPs + L_nZnO), the network, while impacted, retained greater functional integrity and exhibited slightly more resilience compared to low-dose scenario for both MPs and nZnO. Key functions such as C fixation and C degradation remained central but showed slightly lower interaction density than in the high-dose treatment. However, in the L_MPs + H_nZnO network, where low MPs dose combined with high nZnO dose, fewer nodes and positive interactions were preserved as the MPs dose decreased, suggesting that the MPs dose plays a crucial role in determining the extent of microbial network disruption under high nZnO

exposure.

Moreover, networks subjected to combinations of biodegradable-MPs (Bio-MPs, PLA) and conventional-MPs (Con-MPs, including PE and PS) with nZnO showed varying degrees of disruption. Bio-MPs generally maintained slightly more stable interactions compared to synthetic MPs. However, networks treated with Bio-MPs exhibited a shift towards increased negative interactions with microbes, particularly in central functions such as S cycling and human disease-related genes.

4. Discussion

4.1. Impact on microbial diversity and structure

MPs have been shown to cause substantial alterations in soil microbial communities, affecting key ecological metrics such as species richness, diversity, and evenness [12,35,36]. While earlier studies primarily focused on the overall impact of MPs on soil microbial communities or bacterial communities, they often overlooked the responses of less abundant microbial taxa. Understanding these nuanced responses is essential for comprehending the full ecological implications of MPs, particularly in nutrient cycling, organic matter decomposition, and microbial food webs. Here, our study provides the first evidence of differential sensitivity among four distinct microbial groups, i.e., bacteria, archaea, fungi, and viruses, to varying doses and types of MPs, as well as to co-occurring nZnO exposure.

Bacterial communities showed relative resilience in terms of

richness, but metrics such as diversity and evenness were more affected, especially under high doses of biodegradable MPs (10 % PLA). This suggests that while bacterial communities can maintain species richness during environmental stress, their functional diversity and interspecies interactions may be compromised. Bacterial phyla such as Proteobacteria and Actinobacteria are identified as plastic-degrading enriched by MP-amended soils [5,37]. Sun et al. [25] found that these two phyla were dominant bacteria in the rhizosphere of peanut grown in the soil with PE MPs and nZnO. We found that they responded differently to different MPs and nZnO (Table S9). Notably, Proteobacteria increased in relative abundance under PLA exposure, reflecting a sensitive response to MP type ($F=117.18^{***}$). In contrast, Actinobacteria, known for synthetic polymers degradation [38], demonstrated a pronounced positive correlation with traditional MPs (PE and PS). These observations suggest that Proteobacteria may be enriched by PLA additions as fast-growing opportunistic bacteria, whereas Actinobacteria appear to mitigate environmental stress by detoxifying excess polymer pollutants (PE and PS), thereby maintaining the ecological balance.

In contrast to bacteria, less abundant microbial groups, including archaea, fungi, and viruses, exhibited more pronounced responses to MPs. These taxa often possess lower diversity and are more vulnerable to environmental fluctuations, which may explain their heightened sensitivity. Archaeal populations demonstrated a dual response: low nZnO level enhanced richness, but high level, especially when combined with MPs, led to declines. This duality could be indicative of nZnO as both a potential nutrient (providing Zn^{2+}) or stressor, depending on concentration [22]. Significant effects on archaeal phyla Thaumarchaeota and Euryarchaeota indicate that MPs and nZnO can disrupt both nitrification and methanogenesis processes (Table S9). Thaumarchaeota, as ammonia oxidizers, play a key role in the N cycling [39], while Euryarchaeota, including methanogens like *Methanoscincina*, *Methanocella*, and *Methanosaeta*, are critical for methane production under anaerobic conditions. Disruptions in these processes could lead to imbalances in N availability and increased greenhouse gas emissions, which broadens implications for soil health and climate change.

Fungal communities, particularly the phyla Ascomycota and Basidiomycota, play a crucial role in decomposing complex organic materials like cellulose and lignin [40]. In our study, fungal communities exhibited a marked reduction in both richness and diversity under high-dose PLA treatments, indicating significant vulnerability to biodegradable MPs, potentially due to shifts in soil chemistry induced by enhanced biodegradation processes. Ascomycota has been reported to utilize complex carbon sources derived from MPs, showing high abundance and diversity in MPs-polluted soils [5,41]. The strong influence of MPs dose and type on Ascomycota ($F=26.39^{***}$ and $F=29.55^{***}$, respectively; Table S9) suggests that MPs could facilitate the enrichment of plastic-degrading fungi, thereby reducing fungal diversity and richness, aligning with earlier research [42].

Viral communities, though less abundant, exhibited pronounced sensitivity to environmental stressors, with significant declines in both richness and evenness under elevated nZnO doses. Viruses, particularly bacteriophages such as Siphoviridae and Myoviridae, showed strong responses to MPs characteristics and nZnO dose (Table S9). Significant interactions between MPs dose, MPs type, and nZnO indicated that the combined effects of MPs and nZnO can alter virus-induced mortality in bacterial populations. Given that viruses are crucial for modulating microbial population dynamics and facilitating horizontal gene transfer [43], their vulnerability to these pollutants may significantly influence broader microbial community interactions.

4.2. Functional gene responses

4.2.1. Functional categories

Through metagenomic sequencing and statistical analyses, our study offers a comprehensive evaluation of how MPs and nZnO influence the diversity and abundance of functional genes in soil microbial

communities. Strong positive correlations between MPs dose and pathway modules involved in carbohydrate and lipid metabolism, nucleotide and amino acid metabolism, and secondary metabolism suggest that higher doses of MPs may stimulate these essential metabolic processes. This stimulation could be attributed to microbial adaptive responses aimed at mitigating stress or utilizing MPs as alternative carbon sources [38,40], as evidenced by the increasing relative abundance of decomposer phyla, such as Actinobacteria and Ascomycota. Conversely, the negative impact on other modules indicates that certain microbial functions are suppressed under increased MPs doses, potentially due to bio-toxicity [44] or disruption of microbial homeostasis [5]. The type of MPs also significantly influenced various functional modules, notably the pathway module, structural module, and functional sets, implying that different MPs types may alter microbial community functions in distinct ways. These variations may stem from differences in their chemical compositions, surface properties, leached additives, or secondary products [42]. In contrast to MPs, nZnO dose exhibited significant negative effects on both structural and functional modules, indicating a suppressive effect on microbial activities related to energy metabolism and genetic processing. Known for their antimicrobial properties [22], nZnO inhibited energy metabolism pathways, such as ATP synthesis and carbon fixation, suggesting that it impairs fundamental processes essential for microbial survival and ecosystem functioning.

4.2.2. Genes involved in nutrient cycles

Soil microorganisms are central to the functioning of biogeochemical cycles, recycling essential elements through Earth's ecosystems. Our study demonstrated that high doses of nZnO and MPs reduced the abundance of genes for C degradation and N_2 fixation, but increased genes for CO_2 fixation and S metabolism. The diminished abundance of genes involved in C degradation under high-dose nZnO and MPs, particularly PLA, suggests that the dual stress of MPs and nZnO inhibits the microbial enzymatic pathways crucial for breaking down starch, cellulose, hemicellulose, and lignin, which aligns with the findings from Zhang et al. [45] and Yu et al. [46]. A similar decrease in key genes involved in the Calvin cycle further indicated a potential impairment of C assimilation and overall C cycling in microbial communities. Conversely, the unexpected increase in certain CO_2 fixation genes suggests that combinations of MPs and nZnO exert complex, possibly compensatory effects on C degradation and fixation mechanisms within microbial populations. In N cycling, a contrasting pattern was observed: N_2 fixation genes were suppressed, while genes associated with ammonia oxidation and denitrification genes were enriched under elevated PLA and nZnO doses. This shift can be attributed to the changes in soil pH induced by the higher dose of MPs and nZnO, as described in our previous study [24]. As soil pH approaches neutrality, N_2 -fixing microbes, which are typically more sensitive to pH fluctuations, were likely suppressed under slightly alkaline or neutral conditions, leading to a reduction in their abundance. The inhibition of N_2 fixation, along with enhanced activity of nitrification and denitrification processes, could result in incomplete N cycling and greater NH_4^+/NH_3 loss, potentially depleting soil N resources and affecting soil nutrient dynamics.

4.3. Microbial interaction networks

Analysis of microbial interaction networks between soil microbes and genes involved in nutrient cycles further revealed critical insights. High-dose nZnO exposure consistently reduced network complexity, connectivity, and modularity, thereby disrupting nutrient cycling and decreasing ecosystem resilience. Fragmented networks and increased antagonistic interactions rendered the soil ecosystem more vulnerable to stress, ultimately affecting soil fertility and plant growth. However, these negative effects were mitigated by the co-presence of MPs, especially at elevated doses. This mitigation may be attributed to the

influence of MPs on the distribution or bioavailability of nZnO [24–26], though the exact mechanisms require further investigation. Additionally, the increased abundance and connectivity of human disease-related genes under co-exposure to MPs and nZnO suggest a potential rise in pathogenic microbes. This trend can be traced back to the remarkable increase in antibiotic/drug resistance genes (Table S8), as well as the increased abundances of bacteriophages (Fig. 2), indicating a higher propensity for horizontal gene transfer within bacterial communities, ultimately promoting the proliferation of pathogenic microbes.

Networks subjected to combinations of biodegradable MPs and nZnO generally maintained slightly more stable interactions compared to synthetic MPs and nZnO. This may be attributed to the rougher surfaces of PLA MPs, which caused stronger alterations in microbial functional and taxonomic profiles than PE and PS MPs [47]. However, networks treated with biodegradable MPs exhibited a shift toward increased negative interactions between microbes and biochemical genes. This likely results from excess carbon input due to the catabolism of biodegradable MPs, leading to an imbalance in soil nutrient cycling [48]. Thus, while biodegradable MPs may be less disruptive overall, their degradation products or the physicochemical changes induced during decomposition could trigger stress responses or favor the growth of specific microbial groups, such as opportunistic pathogens, potentially compromising ecosystem functions.

4.4. Combined effects of MPs and nZnO

The effects of MPs on soil microbial communities vary widely, with reports indicating positive, negative, or neutral impacts depending on factors such as MP dose, MP type, and the presence of co-contaminants. In the present study, high doses of nZnO were identified as a major driver of these changes, accounting for the greatest proportion of variance in microbial community structure (16.8 %) and nutrient cycling genes (14.3 %), surpassing the effects of MPs dose and type. MPs, particularly at high doses, exacerbate these effects. The greater influence of nZnO likely stems from its smaller size and higher reactivity compared to MPs, enabling easier penetration of microbial cell walls and increased toxicity through Zn²⁺ release. While zinc is essential at low concentrations, elevated Zn²⁺ levels can disrupt cellular processes, leading to reduced microbial diversity. Additionally, nZnO generate ROS, further stressing microbial populations and favoring ROS-resistant species. The combination of Zn²⁺ toxicity, ROS generation, and cell membrane disruption underpins the dominant role of nZnO in shaping microbial communities. Significant two- and three-way interactions among MPs type, MPs dose, and nZnO dose suggest that these pollutants do not act as independent stressors but interact synergistically to influence microbial community composition. Statistical analyses, including PCoA, ANOVA, and Mantel test, reinforced these observations, highlighting the complex interplay between MPs and nZnO in affecting soil microbial ecosystems. Notably, the combined effects of MPs and nZnO involve complex interactions that extend beyond simple additive effects, influencing microbial community structure, functional potential, and ecosystem resilience. Differently, Sun et al. [25] found that PE MPs and nZnO interacted antagonistically on peanut rhizosphere bacterial community diversity. Overall, these intricate consequences highlight that contaminant interactions can lead to unforeseen effects on microbial communities, which cannot be predictable by examining each pollutant in isolation.

In line with previous studies, biodegradable and conventional MPs exhibited differential effects on soil microbial communities [3,48]. These differences are unsurprising given the distinct chemical compositions, degradation rate, surface properties during aging, interaction with the co-existing nZnO, and soil environments among PLA, PE, and PS MPs. In agricultural soil, microbial activity is typically C-limited. Even a small amount of C source can cause soil microbial metabolic changes. In this study, we clearly demonstrated that although PLA is biodegradable, its addition caused adverse effects on soil microbial

communities, including reductions in the abundances of the genes involved in C and N cycling and a decrease in fungal diversity. These changes indicate disruptions in nutrient turnover and essential soil processes, supported by the depletion of soil mineral N observed with the addition of 10 % PLA in our previous study [13]. Moreover, the observed increase in negative interactions among microbes in the presence of PLA points to stress responses or competitive dynamics, which could further destabilize the microbial ecosystem.

These observations suggest that biodegradability does not necessarily equate to ecological harmlessness. Although biodegradable plastics are considered a promising strategy to minimize the risks of MPs residues in soil, their degradation process and interactions with co-existing pollutants could have unintended and potentially adverse ecological consequences. This contrasts with conventional MPs, where such effects appear less pronounced in a short time, possibly due to their inert nature and slower degradation rates. The differential effects observed between biodegradable and conventional MPs raise important questions about the environmental fate and impact of biodegradable plastics. This underscores the need for comprehensive environmental assessments of biodegradable materials, considering not just their biodegradability but also their interactions with soil microbial communities and the potential for unintended ecological consequences.

Finally, soil heterogeneity of pollutants influences microbial community structure and their activity [49,50]. Since MPs and nZnO are both insoluble, soil heterogeneity may still exist even though they were thoroughly mixed into the soil. The platsphere can function as habitats with distinct physicochemical properties and microbial communities compared to the surrounding soil [51]. MPs may recruit specific taxa involved in the biodegradation of the MPs in the platsphere and thus serve as a “special microbial accumulator” [52,53]. Huang et al. [53] found that potential plastic-degrading bacteria (e.g., *Streptomyces*) and pathogens (e.g., *Nocardiaceae*) were highly enriched on PE fragments. Another study observed that bacteria such as *Nocardia*, *Aeromicrobium*, *Amycolatopsis*, and *Rhodococcus* were enriched on the surface of LDPE MPs [54]. Similarly, PE platsphere can also create unique niches for fungi (e.g., *Penicillium* and *Alternaria*) [55]. Particularly, due to different degradability, biodegradable and conventional MPs selected distinct bacteria, fungi, and viruses in their platsphere [56–58]. Notably, the distribution of MPs in soils is highly heterogeneous [29,59], which may further regulate the structure, assembly, functions, and biotic interactions of soil microbiomes. In addition, the environmental behaviors of nZnO may differ in the platsphere and bulk soils, thus resulting in a complex interaction on soil microbiomes. More field experiments are needed to include the heterogeneity of soil MPs and nanoparticles.

5. Conclusion

Our study explored for the first time the impacts of MPs and nZnO on soil microbiomes, demonstrating that MPs and nZnO, both individually and in combination, significantly altered soil microbial taxonomic and functional diversity, with distinct effects based on type and dose. Bacterial communities exhibited higher resilience, while less abundant groups like archaea, fungi, and viruses were more sensitive. High-dose nZnO consistently disrupted microbial network complexity and connectivity, while the co-existence of MPs mitigated part of these negative effects. Furthermore, MPs and nZnO affected genes involved in C, N, P, and S cycling, which can impair nutrient availability and ecosystem function. Conventional MPs (PE and PS) and biodegradable MPs (i.e., PLA) showed distinct effects on microbial taxa, with PLA presenting unique risks, particularly evident in its detrimental effects on fungal communities and microbial interactions. Overall, these findings underscore the complex interactions between MPs and nZnO and highlight the importance of considering their combined environmental risks.

Environmental implication

There are large knowledge gaps in the combined risks of co-existing emerging contaminants in terrestrial ecosystems. This study first highlighted the interaction of microplastics (MPs) and engineered nanoparticles (nZnO) on soil microbiomes, including bacteria, fungi, archaea, and viruses, to reveal their possible disruptions in microbial diversity, functions, and networks. The responses of soil archaea, fungi, and viruses were more sensitive compared to bacteria. Notably, co-existing MPs mitigated nZnO-induced negative effects on microbial networks. The study underscores the need for integrated risk assessments of pollutant interactions, particularly for biodegradable MPs like polylactic acid.

CRediT authorship contribution statement

Sun Jiao: Writing – original draft, Software, Methodology, Formal analysis, Data curation. **Yang Weiwei:** Software, Methodology, Investigation, Formal analysis, Data curation. **Li Mingwei:** Software, Data curation. **Zhang Shuwu:** Methodology, Investigation. **Sun Yuhuan:** Investigation, Formal analysis. **Wang Fayuan:** Writing – review & editing, Supervision, Project administration, Funding acquisition, Conceptualization.

Declaration of Competing Interest

The authors declare that they have no known competing financial interests or personal relationships that could have appeared to influence the work reported in this paper.

Acknowledgments

This work was funded by the Shandong Postdoctoral Science Foundation (SDBX2023028), the Natural Science Foundation of Shandong Province (ZR2020MD120 and ZR2024QD253), and the Project of Shandong Provincial Higher Education Institution Youth Innovation Teams (2023KJ309).

Appendix A. Supporting information

Supplementary data associated with this article can be found in the online version at [doi:10.1016/j.jhazmat.2025.138164](https://doi.org/10.1016/j.jhazmat.2025.138164).

Data availability

Data will be made available on request.

References

- [1] Thompson, R.C., Courtene-Jones, W., Boucher, J., Pahl, S., Raubenheimer, K., Koelmans, A.A., 2024. Twenty years of microplastics pollution research—what have we learned? *Science* 386, eadl2746.
- [2] Shi, R., Liu, W., Lian, Y., Wang, X., Men, S., Zeb, A., et al., 2024. Toxicity mechanisms of nanoplastics on crop growth, interference of phyllosphere microbes, and evidence for foliar penetration and translocation. *Environ Sci Technol* 58, 1010–1021.
- [3] Wang, Q., Feng, X., Liu, Y., Li, W., Cui, W., Sun, Y., et al., 2023. Response of peanut plant and soil N-fixing bacterial communities to conventional and biodegradable microplastics. *J Hazard Mater* 459, 132142.
- [4] Zhao, R., Zuo, Z., Cong, P., Li, H., Li, M., Zhao, Y., et al., 2025. Combined effects of microplastics and Pb on soil-tobacco systems revealed by soil microbiomics and metabolomics. *Pedosphere*. <https://doi.org/10.1016/j.pedsph.2025.03.010>.
- [5] Sun, J., Zhang, X., Gong, X., Sun, Y., Zhang, S., Wang, F., 2024. Metagenomic analysis reveals gene taxonomic and functional diversity response to microplastics and cadmium in an agricultural soil. *Environ Res* 251, 118673.
- [6] Salam, M., Zheng, H., Liu, Y., Zaib, A., Ur Rehman, S.A., Riaz, N., et al., 2023. Effects of micro(nano)plastics on soil nutrient cycling: state of the knowledge. *J Environ Manag* 344, 118437.
- [7] Wang, F., Pei, L., Zhang, S., Sun, J., Han, L., 2024. Microplastics affect ecosystem multifunctionality: increasing evidence from soil enzyme activities. *Land Degrad Dev* 35, 4379–4405.
- [8] Yan, F., Hermansen, C., Zhou, G., Knadel, M., Norgaard, T., 2024. Meta-analysis shows that microplastics affect ecosystem services in terrestrial environments. *J Hazard Mater* 480, 136379.
- [9] Kajal, S., Thakur, S., 2024. Coexistence of microplastics and heavy metals in soil: occurrence, transport, key interactions and effect on plants. *Environ Res* 262, 119960.
- [10] Wang, Y., Feng, Z., Ghani, M.I., Wang, Q., Zeng, L., Yang, X., et al., 2024. Co-exposure to microplastics and soil pollutants significantly exacerbates toxicity to crops: insights from a global meta and machine-learning analysis. *Sci Total Environ* 954, 176490.
- [11] Zhao, S., Rillig, M.C., Bing, H., Cui, Q., Qiu, T., Cui, Y., et al., 2024. Microplastic pollution promotes soil respiration: a global-scale meta-analysis. *Glob Change Biol* 30, e17415.
- [12] Liu, X., Yu, Y., Yu, H., Sarkar, B., Zhang, Y., Yang, Y., et al., 2024. Nonbiodegradable microplastic types determine the diversity and structure of soil microbial communities: a meta-analysis. *Environ Res* 260, 119663.
- [13] Wang, Q., Feng, X., Liu, Y., Cui, W., Sun, Y., Zhang, S., et al., 2022. Effects of microplastics and carbon nanotubes on soil geochemical properties and bacterial communities. *J Hazard Mater* 433, 128826.
- [14] Zhang, S., Pei, L., Zhao, Y., Shan, J., Zheng, X., Xu, G., et al., 2023. Effects of microplastics and nitrogen deposition on soil multifunctionality, particularly C and N cycling. *J Hazard Mater* 451, 131152.
- [15] Ren, X., Tang, J., Liu, X., Liu, Q., 2020. Effects of microplastics on greenhouse gas emissions and the microbial community in fertilized soil. *Environ Pollut* 256, 113347.
- [16] Fan, P., Tan, W., Yu, H., 2022. Effects of different concentrations and types of microplastics on bacteria and fungi in alkaline soil. *Ecotoxicol Environ Saf* 229, 113045.
- [17] Ren, S., Wang, K., Zhang, J., Li, J., Zhang, H., Qi, R., et al., 2023. Potential sources and occurrence of macro-plastics and microplastics pollution in farmland soils: a typical case of China. *Crit Rev Environ Sci Technol* 54, 533–556.
- [18] Chang, J., Fang, W., Liang, J., Zhang, P., Zhang, G., Zhang, H., et al., 2022. A critical review on interaction of microplastics with organic contaminants in soil and their ecological risks on soil organisms. *Chemosphere* 306, 135573.
- [19] Wang, Y., Zhang, G., Zhang, F., Wang, H., 2023. Diagnostic strategy for the combined effects of microplastics and potentially toxic elements on microbial communities in catchment scale. *Sci Total Environ* 860, 160499.
- [20] Hufer, T., Praetorius, A., Wagner, S., von der Kammer, F., Hofmann, T., 2017. Microplastic exposure assessment in aquatic environments: learning from similarities and differences to engineered nanoparticles. *Environ Sci Technol* 51, 2499–2507.
- [21] Ringu, T., Ghosh, S., Das, A., Pramanik, N., 2022. Zinc oxide nanoparticles: an excellent biomaterial for bioengineering applications. *Emergent Mater* 5, 1629–1648.
- [22] Rajput, V.D., Minkina, T.M., Behal, A., Sushkova, S.N., Mandzhieva, S., Singh, R., et al., 2018. Effects of zinc-oxide nanoparticles on soil, plants, animals and soil organisms: a review. *Environ Nanotechnol Monit Manag* 9, 76–84.
- [23] Li, M.R., Liu, F.F., Wang, S.C., Cheng, X., Liu, G.Z., 2020. Phototransformation of zinc oxide nanoparticles and coexisting pollutant: role of reactive oxygen species. *Sci Total Environ* 728, 138335.
- [24] Yang, W., Cheng, P., Adams, C.A., Zhang, S., Sun, Y., Yu, H., et al., 2021. Effects of microplastics on plant growth and arbuscular mycorrhizal fungal communities in a soil spiked with ZnO nanoparticles. *Soil Biol Biochem* 155, 108179.
- [25] Sun, H., Bai, J., Liu, R., Zhao, Z., Li, W., Mao, H., et al., 2024. Polyethylene microplastic and nano ZnO co-exposure: effects on peanut (*Arachis hypogaea* L.) growth and rhizosphere bacterial community. *J Clean Prod* 445, 141368.
- [26] Sun, H., Li, Z., Wen, J., Zhou, Q., Gong, Y., Zhao, X., et al., 2023. Co-exposure of maize to polyethylene microplastics and ZnO nanoparticles: impact on growth, fate, and interaction. *Sci Total Environ* 876, 162705.
- [27] Zhang, S., Ren, S., Pei, L., Sun, Y., Wang, F., 2022. Ecotoxicological effects of polyethylene microplastics and ZnO nanoparticles on earthworm *Eisenia fetida*. *Appl Soil Ecol* 176, 104469.
- [28] Hu, J., He, D., Zhang, X., Li, X., Chen, Y., Wei, G., et al., 2022. National-scale distribution of micro(meso)plastics in farmland soils across China: implications for environmental impacts. *J Hazard Mater* 424, 127283.
- [29] Wang, Y., Hou, P., Liu, K., Hayat, K., Liu, W., 2024. Depth distribution of nano-and microplastics and their contribution to carbon storage in Chinese agricultural soils. *Sci Total Environ* 913, 169709.
- [30] Brown, R.W., Chadwick, D.R., Thornton, H., Marshall, M.R., Bei, S., Distaso, M.A., et al., 2022. Field application of pure polyethylene microplastic has no significant short-term effect on soil biological quality and function. *Soil Biol Biochem* 165, 108496.
- [31] Zang, H., Zhou, J., Marshall, M.R., Chadwick, D.R., Wen, Y., Jones, D.L., 2020. Microplastics in the agroecosystem: Are they an emerging threat to the plant-soil system? *Soil Biol Biochem* 148, 107926.
- [32] Zhou, J., Wen, Y., Marshall, M.R., Zhao, J., Gui, H., Yang, Y., et al., 2021. Microplastics as an emerging threat to plant and soil health in agroecosystems. *Sci Total Environ* 787, 147444.
- [33] Chen, M., Zhao, X., Wu, D., Peng, L., Fan, C., Zhang, W., et al., 2022. Addition of biodegradable microplastics alters the quantity and chemodiversity of dissolved organic matter in latosol. *Sci Total Environ* 816, 151960.
- [34] Wang, F., Adams, C.A., Shi, Z., Sun, Y., 2018. Combined effects of ZnO NPs and Cd on sweet sorghum as influenced by an arbuscular mycorrhizal fungus. *Chemosphere* 209, 421–429.

- [35] Feng, X., Wang, Q., Sun, Y., Zhang, S., Wang, F., 2022. Microplastics change soil properties, heavy metal availability and bacterial community in a Pb-Zn-contaminated soil. *J Hazard Mater* 424, 127364.
- [36] Xu, S., Zhao, R., Sun, J., Sun, Y., Xu, G., Wang, F., 2024. Microplastics change soil properties, plant performance, and bacterial communities in salt-affected soils. *J Hazard Mater* 471, 134333.
- [37] Qiu, G., Wang, Q., Wang, Q., Wang, T., Kang, Z., Zeng, Y., et al., 2023. Effects of polyethylene microplastics on properties, enzyme activities, and the succession of microbial community in Mollisol: at the aggregate level. *Environ Res* 237, 116976.
- [38] Zhu, F., Yan, Y., Doyle, E., Zhu, C., Jin, X., Chen, Z., et al., 2022. Microplastics altered soil microbiome and nitrogen cycling: the role of phthalate plasticizer. *J Hazard Mater* 427, 127944.
- [39] Biggs-Weber, E., Aigle, A., Prosser, J.I., Gubry-Rangin, C., 2020. Oxygen preference of deeply-rooted mesophilic thaumarchaeota in forest soil. *Soil Biol Biochem* 148, 107848.
- [40] Manici, L.M., Caputo, F., De Sabata, D., Fornasier, F., 2024. The enzyme patterns of Ascomycota and Basidiomycota fungi reveal their different functions in soil. *Appl Soil Ecol* 196, 105323.
- [41] Rüthi, J., Rast, B.M., Qi, W., Perez-Mon, C., Pardi-Comensoli, L., Brunner, I., et al., 2023. The plastisphere microbiome in alpine soils alters the microbial genetic potential for plastic degradation and biogeochemical cycling. *J Hazard Mater* 441, 129941.
- [42] Aralappanavar, V.K., Mukhopadhyay, R., Yu, Y., Liu, J., Bhatnagar, A., Praveena, S. M., et al., 2024. Effects of microplastics on soil microorganisms and microbial functions in nutrients and carbon cycling - a review. *Sci Total Environ* 924, 171435.
- [43] Shapiro, O.H., Kushmaro, A., Brenner, A., 2010. Bacteriophage predation regulates microbial abundance and diversity in a full-scale bioreactor treating industrial wastewater. *ISME J* 4, 327–336.
- [44] Luo, H., Liu, C., He, D., Xu, J., Sun, J., Li, J., et al., 2022. Environmental behaviors of microplastics in aquatic systems: a systematic review on degradation, adsorption, toxicity and biofilm under aging conditions. *J Hazard Mater* 423, 126915.
- [45] Zhang, Y., Li, X., Xiao, M., Feng, Z., Yu, Y., Yao, H., 2022. Effects of microplastics on soil carbon dioxide emissions and the microbial functional genes involved in organic carbon decomposition in agricultural soil. *Sci Total Environ* 806, 150714.
- [46] Yu, Y., Li, X., Feng, Z., Xiao, M., Ge, T., Li, Y., et al., 2022. Polyethylene microplastics alter the microbial functional gene abundances and increase nitrous oxide emissions from paddy soils. *J Hazard Mater* 432, 128721.
- [47] Hu, X., Gu, H., Sun, X., Wang, Y., Liu, J., Yu, Z., et al., 2023. Distinct influence of conventional and biodegradable microplastics on microbe-driving nitrogen cycling processes in soils and plasti-spheres as evaluated by metagenomic analysis. *J Hazard Mater* 451, 131097.
- [48] Zhou, J., Gui, H., Banfield, C.C., Wen, Y., Zang, H., Dippold, M.A., et al., 2021. The microplasti-sphere: biodegradable microplastics addition alters soil microbial community structure and function. *Soil Biol Biochem* 156, 108211.
- [49] Mukherjee, S., Juottonen, H., Siivonen, P., Quesada, C.L., Tuomi, P., Pulkkinen, P., et al., 2014. Spatial patterns of microbial diversity and activity in an aged creosote-contaminated site. *ISME J* 8, 2131–2142.
- [50] Becker, J.M., Parkin, T., Nakatsu, C.H., Wilbur, J.D., Konopka, A., 2006. Bacterial activity, community structure, and centimeter-scale spatial heterogeneity in contaminated soil. *Micro Ecol* 51, 220–231.
- [51] Rillig, M.C., Kim, S.W., Zhu, Y.G., 2023. The soil plasti-sphere. *Nat Rev Microbiol* 22, 64–74.
- [52] Zhang, M., Zhao, Y., Qin, X., Jia, W., Chai, L., Huang, M., et al., 2019. Microplastics from mulching film is a distinct habitat for bacteria in farmland soil. *Sci Total Environ* 688, 470–478.
- [53] Huang, Y., Zhao, Y., Wang, J., Zhang, M., Jia, W., Qin, X., 2019. LDPE microplastic films alter microbial community composition and enzymatic activities in soil. *Environ Pollut* 254, 112983.
- [54] Ya, H., Xing, Y., Zhang, T., Lv, M., Jiang, B., 2022. LDPE microplastics affect soil microbial community and form a unique plasti-sphere on microplastics. *Appl Soil Ecol* 180, 104623.
- [55] Sun, Y., Xie, S., Zang, J., Wu, M., Tao, J., Li, S., et al., 2024. Terrestrial plasti-sphere as unique niches for fungal communities. *Commun Earth Environ* 5, 483.
- [56] Li, K., Jia, W., Xu, L., Zhang, M., Huang, Y., 2023. The plasti-sphere of biodegradable and conventional microplastics from residues exhibit distinct microbial structure, network and function in plastic-mulching farmland. *J Hazard Mater* 442, 130011.
- [57] Li, K., Xu, L., Bai, X., Zhang, G., Zhang, M., Huang, Y., 2024. Differential fungal assemblages and functions between the plasti-sphere of biodegradable and conventional microplastics in farmland. *Sci Total Environ* 906, 167478.
- [58] Kutralam-Muniasamy, G., Shruti, V.C., Pérez-Guevara, F., 2024. Plasti-sphere-hosted viruses: a review of interactions, behavior, and effects. *J Hazard Mater* 472, 134533.
- [59] Liu, Y., Rillig, M.C., Liu, Q., Huang, J., Khan, M.A., Li, X., et al., 2023. Factors affecting the distribution of microplastics in soils of China. *Front Environ Sci Engin* 17, 110.